Metal-Directed Stereoselective Syntheses of Homochiral Complexes of *exo*-Bidentate Binaphthol Derivatives

Ruihu Wang,[a,b] Lijin Xu,[a] Jianxin Ji,[a] Qian Shi,[a,b] Yueming Li,[a] Zhongyuan Zhou,[a] Maochun Hong,*[b] and Albert S. C. Chan*[a]

Keywords: Cadmium / N ligands / Palladium / Silver / Zinc

The homochiral *exo*-bidentate ligands (*S*)-2,2′-bis(pyridylmethyleneoxy)-1,1′-binaphthyl [(*S*)-L] and (*R*)-2,2′-bis(pyridylmethyleneoxy)-1,1′-binaphthyl [(*R*)-L] were synthesized and employed for the preparation of coordination complexes with the aim of investigating the effect of an axially chiral 1,1′-binaphthyl connector on self-assembly process. Five homochiral complexes, $[Ag\{(S)\text{-}L\}(ClO_4)]_n$ (**1**), $[Ag\{(R)\text{-}L\}(ClO_4)]_n$ (**2**), $[\{Cd\{(S)\text{-}L\}(H_2O)Cl_2\}(H_2O)_{0.5}]_n$ (**3**), $[(Zn\{(S)\text{-}L\}Cl_2)(DMF)_{0.5}(H_2O)_{0.5}]_n$ (**4**), and $[(Pd_2\{(S)\text{-}L\}_2Cl_4)(H_2O)_{1.5}]_n$ (**5**), have been prepared and characterized by single-crystal X-ray diffraction analyses. The enantiomeric complexes **1** and **2** are isomorphous and are formed through interconnection of ligands and two-coordinate Ag^I centers. Complex **3** possesses a similar structural framework to **1** and is formed with two nitrogen atoms from (*S*)-L coordinating to six-coordinate Cd^{II} in a *trans* mode. The interlocking in part of the adjacent, one-dimensional helix-like chains stabilizes its structure. Complex **4** is a one-dimensional zigzag chain and is formed through interconnection of (*S*)-L and $ZnCl_2$ units. The *exo*-bidentate (*S*)-L ligand in **5** links square-planar Pd^{II} into a homochiral dinuclear metallomacrocycle.

Introduction

The design and construction of well-defined supramolecular architectures through metal-directed self-assembly of metal ions and organic ligands or organometallic substances are important for developing rational approaches to prepare novel metallosupramoleclues with intriguing structural and functional features.[1–4] In this context, the selection of multifunctional organic ligands containing appropriate coordination sites linked by a connector with specific positional orientation and/or functionality is especially crucial.[3,4] Various ligands have been tailored to recognize the intrinsic geometric preferences of specific metal ions or to encode structural constraints upon their coordination to metal ions. Metal–pyridine coordination has proved to be an excellent tool in self-assembly as it is strongly affected by the structural characteristics of the connector groups between the organic bridging ligands and the metal ions. Many pyridine-donor bis-monodentate ligands interconnected by rigid or flexible connectors, such as alkyl[5] or aryl groups,[6] or even organometallic complexes,[7] have been employed to construct metal-organic frameworks. Thus, it is of high interest to establish the rules that control the self-assembly process through chemical programming of suitable components and assembly algorithms.

In our previous study, we prepared a series of pyridine-donor ligands by connecting methylsulfanylpyridyl to aromatic ring connectors; the assembly of such ligands and metal ions resulted in several unique structural motifs, such as a metallosupramolecular cube,[8a] a one-dimensional nanotube,[8b] a dimetallomacrocycle,[8c] square rings with guest molecules,[8d] and a two-dimensional crown-like structure.[8d,8e] From the viewpoint of constructing functional complexes, it may be more valuable to introduce functionalized chiral groups directly into *exo*-bidentate pyridyl ligands as connectors instead of using nonfunctional connectors. Optically active 1,1′-bi-2-naphthol (BINOL) derivatives have been extensively applied to asymmetric synthesis and molecular recognition owing to their conformational stability and molecular flexibility.[9] Moreover, BINOL is also a good chiral connector for the design of new pyridine-donor ligands and the construction of novel, chiral, conjugated materials and fluorescent sensors.[10] We have recently investigated the effect of an axially chiral BINOL backbone on the self-assembly process through the introduction of an optically active BINOL backbone into *exo*-bidentate pyridyl ligands. The preliminary results indicated that the rigidity of the binaphthyl backbone facilitates the transfer of chiral information.[9d] In an effort to elucidate the effect of the coordination geometry of the metal ions on the self-

[a] Open Laboratory of Chirotechnology, Department of Applied Biology and Chemical Technology, The Hong Kong Polytechnic University,
Hong Hum, Hong Kong
Fax: +852-2364-9932
E-mail: bcachan@polyu.edu.hk
[b] State Key Laboratory of Structural Chemistry, Fujian Institute of the Research on the Structure of Matter, Chinese Academy of Sciences,
Fuzhou, Fujian, 350002, China

assembly process, we report herein the syntheses and characterizations of a series of homochiral complexes {[Ag{(*S*)-L}(ClO_4)]$_n$ (**1**), [Ag{(*R*)-L}(ClO_4)]$_n$ (**2**), [{Cd{(*S*)-L}(H_2O)Cl_2}(H_2O)$_{0.5}$]$_n$ (**3**), [(Zn{(*S*)-L}Cl_2)(DMF)$_{0.5}$(H_2O)$_{0.5}$]$_n$ (**4**), and [(Pd_2){(*S*)-L}$_2Cl_4$)(H_2O)$_{1.5}$]$_n$ (**5**) [(*S*)-L = (*S*)-2,2′-bis(pyridylmethyleneoxy)-1,1′-binaphthalene; (*R*)-L = (*R*)-2,2′-bis(pyridylmethyleneoxy)-1,1′-binaphthalene], in which Ag^I, Cd^{II}, Zn^{II}, and Pd^{II} adopt distorted linear, octahedral, tetrahedral, and square-planar geometries, respectively.

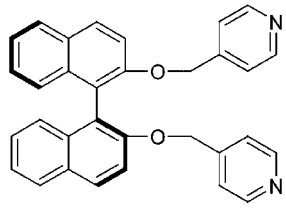

(*S*)-L

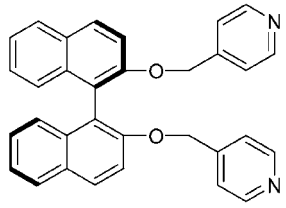

(*R*)-L

Results and Discussion

Syntheses

The reaction of (*S*)-1,1′-bi-2-naphthol or (*R*)-1,1′-bi-2-naphthol with 4-picolyl chloride hydrochloride was first carried out in the presence of K_2CO_3 in refluxing acetone under nitrogen for three days to afford *exo*-bidentate (*S*)-L or (*R*)-L in low yields (ca. 15%). The main product of the reaction was a mono-substituted compound (ca. 72%). However, when NaOH was used as the base under the same reaction conditions, (*S*)-L or (*R*)-L was obtained in high yield (88%). These results indicate that the base has a great effect on the yield of (*S*)-L or (*R*)-L. The specific optical rotations of (*S*)-L and (*R*)-L are –54.44° and 54.51° ($[\alpha]_D^{20}$, *c* = 1, THF), respectively. In comparison, the specific optical rotations of (*S*)- and (*R*)-1,1′-bi-2-naphthol are –35.50° and 35.50° ($[\alpha]_D^{20}$, *c* = 1, THF), respectively, thus indicating that the methylpyridine-donor groups in the ligands affect the chiral twist of BINOL. The ligands (*S*)-L and (*R*)-L are soluble in most organic solvents. The reaction of (*S*)-L or (*R*)-L with $AgClO_4$ in a 1:1 molar ratio in MeCN/H_2O (2:1) led to the formation of the corresponding enantiomeric complex **1** or **2**, respectively. As anticipated for (*S*) and (*R*) enantiomers, **1** and **2** possess the same structural framework and equal but opposite optical rotation. It is well known that the coordination geometry of metal ions plays an important role in the construction of supramolecular architectures. Hence, the successful syntheses of **1** and **2** prompted us to go beyond the two-coordinate Ag^I to metal ions of high coordination numbers. The reaction of (*S*)-L with $CdCl_2$ or $ZnCl_2$ in MeCN/H_2O afforded precipitates that were not soluble in any solvent. When a MeOH solution of (*S*)-L was layered on top of an aqueous solution of $CdCl_2$, suitable single crystals were formed. However, crystals of lower quality were produced using $ZnCl_2$ instead of $CdCl_2$ under the same conditions. In contrast, the diffusion of diethyl ether into a DMF/MeCN solution of (*S*)-L and $ZnCl_2$ resulted in crystals suitable for an X-ray single-crystal diffraction study.

Structural Description

[Ag{(S)-L}(ClO_4)]$_n$ (1) and [Ag{(R)-L}(ClO_4)]$_n$ (2)

As anticipated, the enantiomeric complexes **1** and **2** are isomorphous. The single-crystal X-ray structural analyses reveal that they consist of one-dimensional, helix-like chains formed through interconnection of two-coordinate Ag^I centers and homochiral ligands. As shown in Figure 1, Ag^I is in a distorted linear geometry and is coordinated by two nitrogen atoms from different ligands. The Ag–N bond distances (Table 1) are in the range of 2.157(4)–2.162(4) Å, which are typical values for Ag^I–N_{py} coordination distances.[8b,8c] The N(1)–Ag–N(2A) bond angle of 172.65(1)° in **2** is slightly smaller than that of 175.34(15)° in **1**. (*S*)-L in **1** and (*R*)-L in **2** bind in an *exo*-bidentate mode to bridge a pair of adjacent Ag^I centers. As shown in Table 2, the dihedral angles between two naphthyl rings of (*S*)-L and (*R*)-L are 69.3° and 69.8°, respectively, which are approximately equal, thus indicating that the BINOL backbone has hardly been affected. The dihedral angles between the naphthyl rings and their corresponding pyridyl rings are 41.9° and 87.7°, respectively, in **1**. The corresponding angles are 45.1° and 85.6°, respectively, in **2**. The distance between two Ag^I centers bridged by (*S*)-L and (*R*)-L are 4.74 and 4.69 Å, respectively, while the closest distances between two Ag^I centers unsupported by (*S*)-L, (*R*)-L, or the other molecular interactions are 7.28 and 7.32 Å in **1** and **2**, respectively. These slight differences are probably due to packing effects. It is noteworthy that two adjacent homochiral ligands on the same side produce a cleft with the same mean distance of 7.15 Å for **1** and **2**. This dimension is sufficient to recognize suitable aromatic guest molecules. The moiety of ligands in the adjacent helical chains is interlocked into the cleft of each other (Figure 1). The ClO_4^- counteranion, which lies inside the cleft in part through a weak interaction with Ag^I, further fills the void around the metal ions.

[(Cd{(S)-L}(H_2O)Cl_2)(H_2O)$_{0.5}$]$_n$ (3)

Complex **3** is a one-dimensional, left-handed, helix-like chain formed through the interconnection of (*S*)-L and six-coordinate Cd^{II}. As shown in Figure 2, each Cd^{II} center is coordinated by two nitrogen atoms from different (*S*)-L ligands in the apical positions [N(1)–Cd–N(2A) bond angle of 174.6(3)°; Table 1], with two bridging Cl^- ligands in a *cis* mode, a terminal Cl^-, and a water molecule occupying the

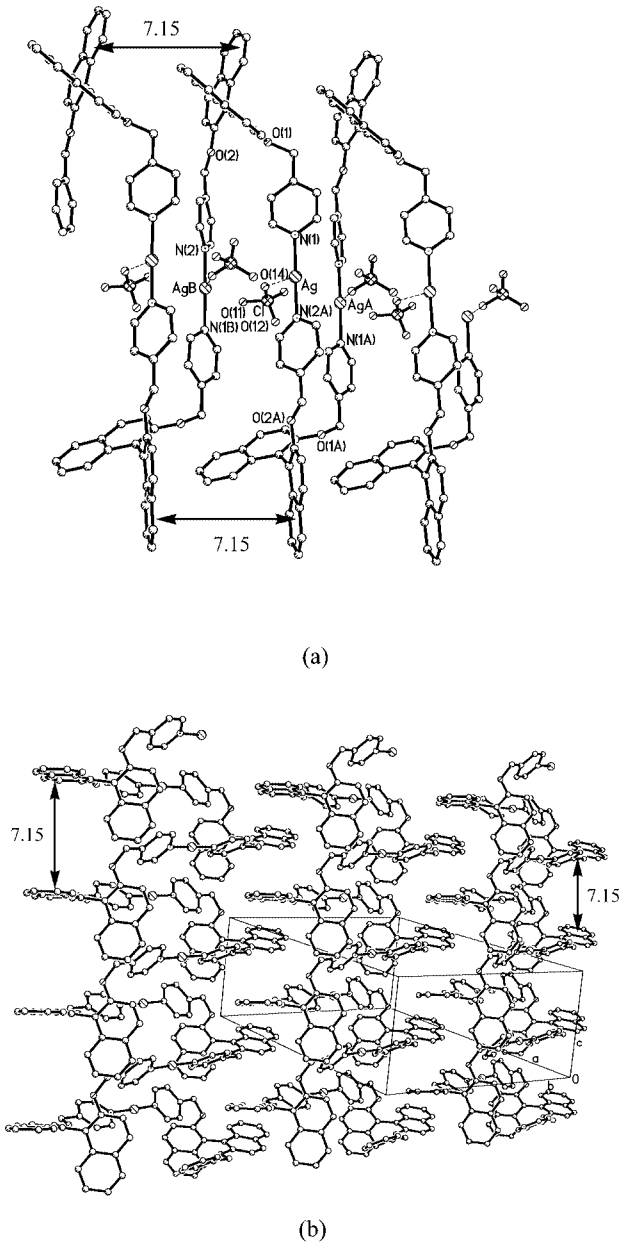

Figure 1. (a) View of the left-handed, helix-like chain in **1**; (b) packing diagram showing inter-immersion of adjacent chains in the clefts in **1** along the (210) direction

Table 1. Selected bond lengths [Å] and angles [°] for complexes **1**–**5**

Complex **1**[a]			
Ag–N(1)	2.162(4)	Ag–O(14)	2.891(12)
Ag–N(2A)	2.157(4)		
N(2A)–Ag–N(1)	175.34(15)	N(1)–Ag–O(14)	85.1(5)
N(2A)–Ag–O(14)	99.5(5)		
Complex **2**[b]			
Ag–N(1)	2.162(4)	Ag–O(12)	2.812(12)
Ag–N(2A)	2.175(4)	Ag–O(12B)	2.813(11)
N(1)–Ag–N(2A)	172.65(17)	N(1)–Ag–O(12B)	90.8(3)
N(1)–Ag–O(12)	93.5(4)	N(2A)–Ag–O(12B)	96.4(4)
N(2A)–Ag–O(12)	86.5(4)	O(12)–Ag–O(12B)	102.6(3)
Complex **3**[c]			
Cd–N(2A)	2.319(4)	Cd–Cl(2)	2.540(2)
Cd–N(1)	2.333(4)	Cd–Cl(1)	2.650(2)
Cd–O(1W)	2.401(5)	Cd–Cl(1B)	2.732(2)
N(2A)–Cd–N(1)	174.6(3)	O(1W)–Cd–Cl(1)	171.03(12)
N(2A)–Cd–O(1W)	92.1(2)	Cl(2)–Cd–Cl(1)	100.80(7)
N(1)–Cd–O(1W)	85.9(2)	N(2A)–Cd–Cl(1B)	85.53(14)
N(2A)–Cd–Cl(2)	92.20(13)	N(1)–Cd–Cl(1B)	89.17(13)
N(1)–Cd–Cl(2)	92.77(12)	O(1W)–Cd–Cl(1B)	82.36(13)
O(1W)–Cd–Cl(2)	86.88(14)	Cl(2)–Cd–Cl(1B)	168.91(7)
N(2A)–Cd–Cl(1)	92.2(2)	Cl(1)–Cd–Cl(1B)	90.14(3)
N(1)–Cd–Cl(1)	89.0(2)	Cd–Cl(1)–Cd(A)	142.52(7)
Complex **4**[d]			
Zn–N(1)	2.006(8)	Zn–Cl(1)	2.217(3)
Zn–N(2A)	2.026(8)	Zn–Cl(2)	2.223(3)
N(1)–Zn–N(2A)	104.1(3)	N(1)–Zn–Cl(2)	107.0(3)
N(1)–Zn–Cl(1)	105.3(3)	N(2A)–Zn–Cl(2)	110.6(2)
N(2A)–Zn–Cl(1)	103.9(3)	Cl(1)–Zn–Cl(2)	124.2(1)
Complex **5**			
Pd(1)–N(1)	2.021(3)	Pd(1)–N(4)	2.032(3)
Pd(2)–N(2)	1.998(3)	Pd(2)–N(3)	2.000(3)
Pd(1)–Cl(1)	2.2914(19)	Pd(1)–Cl(2)	2.315(2)
Pd(2)–Cl(3)	2.302(2)	Pd(2)–Cl(4)	2.292(2)
N(4)–Pd(1)–N(1)	172.88(11)	Cl(1)–Pd(1)–Cl(2)	174.32(9)
N(4)–Pd(1)–Cl(1)	87.15(11)	N(1)–Pd(1)–Cl(1)	88.54(8)
N(4)–Pd(1)–Cl(2)	89.84(11)	N(1)–Pd(1)–Cl(2)	94.92(9)
N(2)–Pd(2)–N(3)	173.29(13)	Cl(3)–Pd(2)–Cl(4)	174.47(10)
N(2)–Pd(2)–Cl(3)	91.65(11)	N(3)–Pd(2)–Cl(3)	91.79(12)
N(2)–Pd(2)–Cl(4)	89.06(11)	N(3)–Pd(2)–Cl(4)	88.07(11)

[a] Symmetry codes: (A) $-x + 1/2$, $y - 1/2$, $-z + 1$. [b] Symmetry codes: (A) $-x + 3/2$, $y + 1/2$, $-z + 2$; (B) $-x + 3/2$, $y - 1/2$, $-z + 2$. [c] Symmetry codes: (A) $-x + 1/2$, $y + 1/2$, $-z + 1$; (B) $-x + 1/2$, $y - 1/2$, $-z + 1$. [d] Symmetry codes: (A) $x + 1$, y, z.

equatorial plane. Thus, the coordination environment around Cd^{II} can best be described as a distorted Cl_3N_2O octahedron, which is rare in Cd^{II} complexes. Cd^{II} is approximately coplanar with the atoms in the equatorial plane, with a slight deviation of 0.027 Å. (*S*)-L serves as an *exo*-bidentate ligand, and the dihedral angles between the two naphthyl rings is 110.1°, which is close to those in **1** and **2**. However, the dihedral angle between the naphthyl rings and their corresponding pyridyl rings are 37.4° and 94.9°, respectively (Table 2). Thus, the interconnections of (*S*)-L and the six-coordinate Cd^{II} centers form a one-dimensional, helix-like chain similar to complex **1**. The Cd···Cd distance bridged by (*S*)-L and Cl^- is 5.10 Å. The uncoordinated water molecules stabilize the helix-like chain through hydrogen-bonding interactions between the uncoordinated water molecule and the coordinated water molecule [O(2W)···O(1W)^i = 2.797(12) Å; symmetry code: (i) x, $y + 1$, z,] as well as between the uncoordinated water molecule and terminal Cl^- [Cl(2)···H–O(2) = 3.129(11) Å]. It is noteworthy that the uncoordinated water molecule, coordinated water molecule, terminal Cl^-, and Cd^{II} form a trimetallocentered ten-membered hydrogen bonding ring. The Cd···Cd separation formed by uncoordinated water molecules through hydrogen-bonding interaction is 7.18 Å. The clefts from two adjacent (*S*)-L ligands are 7.04 Å, which is smaller than that in **1**. The complementary interlocking in part of the adjacent chains further stabilizes the chain by efficiently filling the void of the clefts (see b in Figure 2).

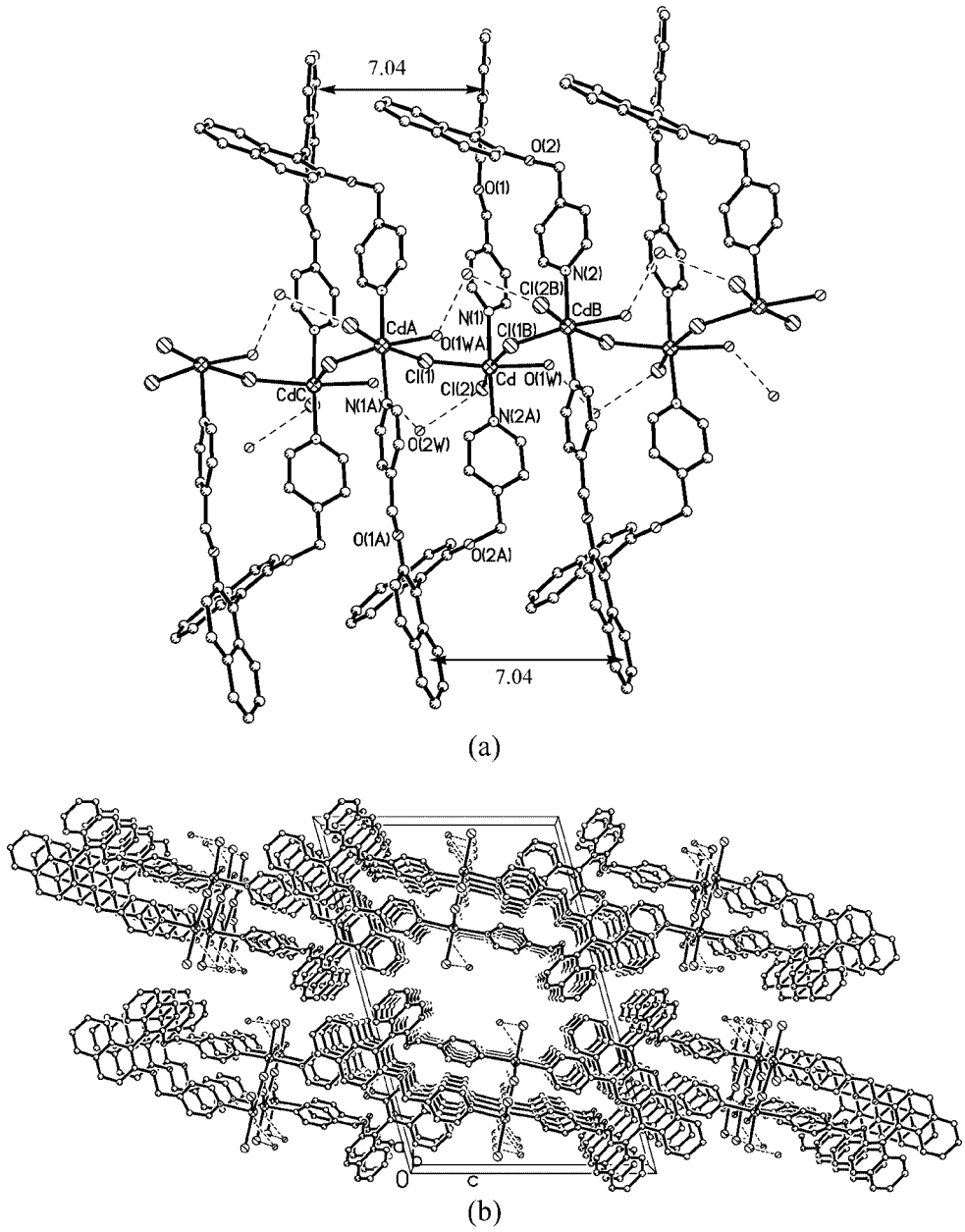

Figure 2. (a) View of the right-handed, helix-like chain in **3**; (b) view of the packing diagram of inter-immersed adjacent chains along the *b* axis

Table 2. A comparison of the structural data of the homochiral ligands in complexes **1**–**5**

Compound	Dihedral angles [°]				Distance between metal centers bridged by ligand [Å]	Structure
	Binaphthyl rings	Naphthyl ring and its pyridyl ring	Two pyridyl rings in the ligand	Two pyridyl rings at metal center		
1	69.3	41.9 and 87.7	85.4	21.6	4.74	1D helix-like chain
2	69.8	45.1 and 85.6	88.2	24.1	4.69	1D helix-like chain
3	69.9	37.3 and 85.1	83.8	27.1	5.10	1D helix-like chain
4	85.1	29.3 and 13.3	84.5	84.5	11.30	1D polymeric chain
5	81.7	30.1 and 64.8	82.4	45.5	4.644	dimetallomacrocycle

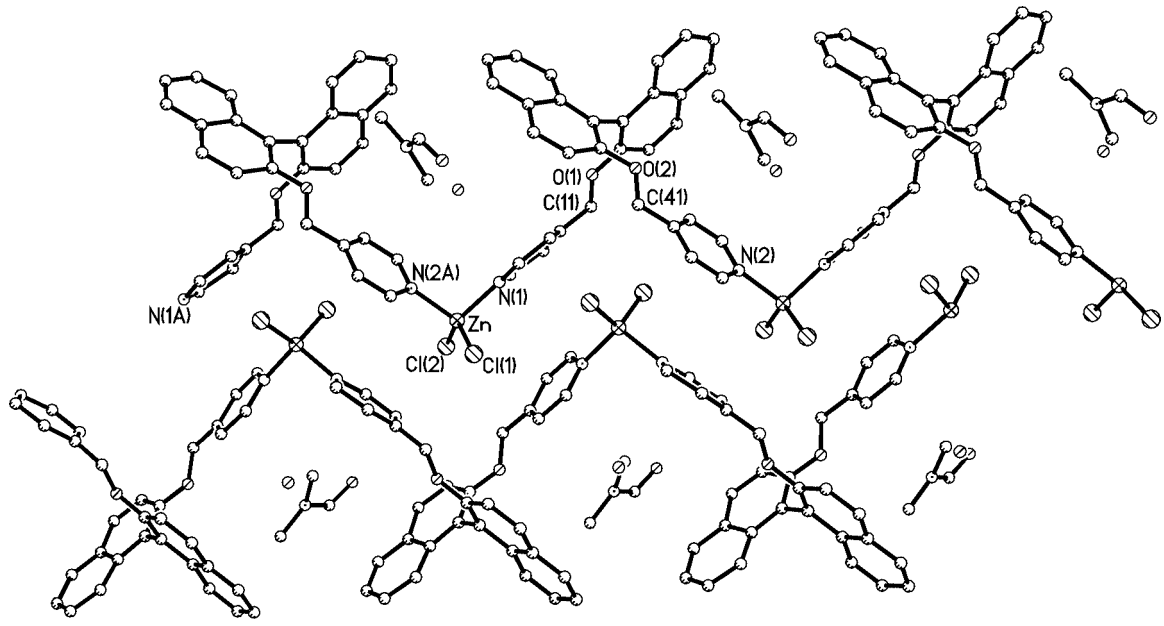

Figure 3. View of the double zigzag chains with guest DMF and water molecules in **4** along the *c* axis

[(Zn{(S)-L}Cl$_2$)(DMF)$_{0.5}$(H$_2$O)$_{0.5}$]$_n$ (4)

The single-crystal X-ray structural analysis reveals that **4** consists of a one-dimensional zigzag chain formed through the interconnection of $ZnCl_2$ units and (*S*)-L. As shown in Figure 3, each Zn^{II} ion is in a distorted tetrahedral geometry and is coordinated by two terminal Cl^- and two nitrogen atoms from different (*S*)-L ligands [Zn–N = 2.006(8) and 2.026(8) Å; N(1)–Zn–N(2A) = 104.1(3)°; Table 1]. The dihedral angle between two pyridyl rings attached to Zn^{II} is 84.5°, thus confirming the approximately perpendicular arrangement of the two coordinated pyridyl rings. All (*S*)-L ligands bind in an *exo*-bidentate mode and lie on the same side of the polymer chain, which is very different from the situation in **1**–**3**. The pyridyl rings are twisted around their naphthyl rings, with the dihedral angles between them being 13.3° and 29.3°, respectively (Table 2). A dramatic twisting between the two naphthyl rings is also observed, with the dihedral angle between them being 76.2°, which is larger than those in **1**–**3**. The combination of these twistings makes the (*S*)-L-connected $ZnCl_2$ units form a one-dimensional polymeric chain. The adjacent Zn···Zn separation bridged by (*S*)-L is 11.30 Å. The other chain with the same chirality fills the chain void between $ZnCl_2$ units in a complementary fashion to stabilize the chain structure. The DMF and water molecules, which lie outside the open cavity formed by the adjacent (*S*)-L ligands, do not generate significant weak interactions.

[(Pd$_2${(S)-L}$_2$Cl$_4$)(H$_2$O)$_{1.5}$]$_n$ 5

Complex **5** has a homochiral, binuclear metallocyclic structure. As shown in Figure 4, both Pd(1) and Pd(2) are in a distorted square-planar geometry and are coordinated by two *trans*-pyridine nitrogen atoms of different (*S*)-L and two *trans* Cl^- ligands, with *cis* angles ranging from 87.7(3)° to 94.9(3)° (Table 1). The average bond distances of Pd–N_{py} and Pd–Cl are 2.008(12) Å and 2.305(4) Å, respectively, which are typical values for Pd–N_{py} and Pd–Cl bond lengths. (*S*)-L acts as an *exo*-bidentate ligand, with its pyridyl rings slightly twisted with respect to their naphthyl rings, with the dihedral angles between them being 30.1° and 64.8° and 29.3° and 87.9°, respectively. The two naphthyl rings are also drastically twisted, with the dihedral angle between them being 81.7° and 82.7°, respectively. The combination of these twistings allows the (*S*)-L ligands to link the $PdCl_2$ units into a thirty-four-membered bimetallic macrocycle. The Pd···Pd separation in the cycle is 4.644 Å. Owing to the high distortion and flexibility of (*S*)-L, no enclathration of guest molecules is observed in **5**; the uncoordinated water molecules lie outside of the macrocycle. There are no other significant weak interactions or short contacts between the adjacent macrocycles.

It is of interest to compare the related structural data of (*S*)-L or (*R*)-L in **1**–**5**. (*S*)-L and (*R*)-L act as *exo*-bidentate ligands, and the difference of the coordinating geometry of the metal ions in **1**–**5** results in different structural topologies. In complexes **1** and **2**, owing to the configurational difference, (*S*)-L and (*R*)-L bridge two-coordinate Ag^I generating left-handed and right-handed helix-like chains, respectively. The frameworks of (*S*)-L and (*R*)-L are not crucially affected by the coordination to metal centers, as shown by the data in Table 2. In complex **3**, two nitrogen atoms from different (*S*)-L ligands occupy the axial positions of a six-coordinate Cd^{II} center, which results in a structural framework similar to **1**. Thus, the dihedral angles between the two naphthyl rings are very close and are the smallest in **1**–**5**. The slight difference between the one-dimensional, helix-like chains is due to free rotation of methylpyridine. However, the distortion angle of the BINOL connector in **4**

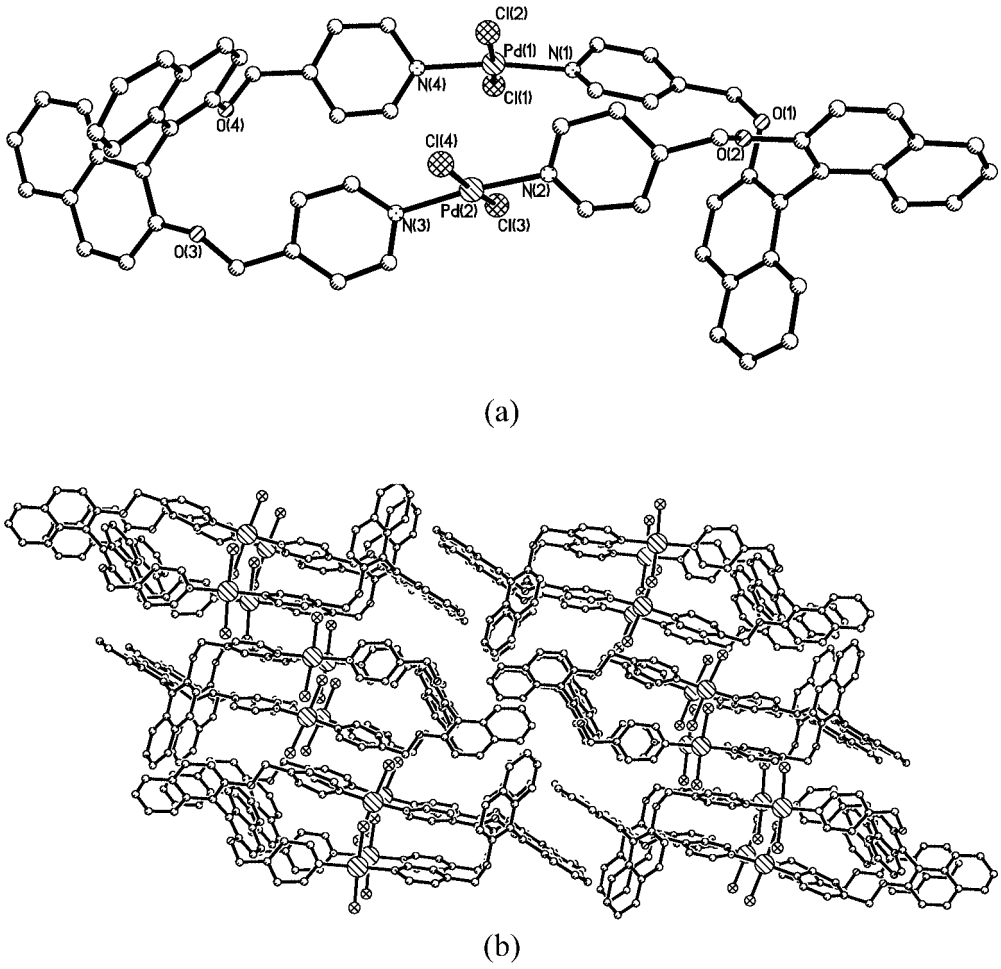

Figure 4. (a) View of the molecular structure of **5**, with uncoordinated water molecules omitted for clarity; (b) view of the packing structure along the *b* axis in **5** showing that there are no other interactions between adjacent macrocycles

(85.1°) is larger than those in **1** and **3**, which results in the formation of a one-dimensional zigzag chain with the (*S*)-L ligands on the same side, with the largest distance between metal centers bridged by (*S*)-L (11.30 Å). The shortest distance is found in dinuclear metallomacrocyclic complex **5** (4.644 Å), in which two Pd^{II} centers are bridged by two (*S*)-L ligands. Therefore, the combination of both the structural characteristics of the BINOL connector and the coordination propensity of the metal ions leads to the formation of the final frameworks of complexes **1**–**5**.

Conclusions

We have successfully synthesized the BINOL-based, homochiral, pyridyl-containing ligands (*S*)-2,2′-bis(pyridylmethyleneoxy)-1,1′-binaphthalene [(*S*)-L] and (*R*)-2,2′-bis(pyridylmethyleneoxy)-1,1′-binaphthalene [(*R*)-L]. Each ligand binds in an *exo*-bidentate mode to bridge two adjacent metal centers. In complexes **1**–**3**, the ligands on different sides link two-coordinate Ag^{I} centers (**1** and **2**) and six-coordinate Cd^{II} centers (**3**) into homochiral helix-like chains, which are stabilized through complementary interlocking in parts of the adjacent chains. In the four-coordinate Zn^{II} complex **4**, the (*S*)-L ligands on the same side link $ZnCl_2$ units into a zigzag chain and the zigzag is stabilized by interlocking with the other chain. However, in the square-planar Pd^{II} complex **5**, the (*S*)-L ligands link *trans*-coordinated $PdCl_2$ units into a homochiral dinuclear metallomacrocycle. The dihedral angle between the two naphthyl rings of the BINOL connector is different in the different structural topologies, thus suggesting that the coordination geometry of the metal ions has an important effect on the framework twisting of the BINOL moiety. It should be noted that the metal ions themselves cannot be considered to be the center of chirality in **1**–**5** as the chirality of these complexes originates from the inherently chiral twisting in the BINOL connector. Thus, assembly of (*S*)-L with Ag^{I} and Cd^{II} results in the formation of left-handed, helix-like complexes **1** and **3**, respectively Correspondingly, the assembly of (*R*)-L with Ag^{I} leads to the formation of the right-handed, helix-like complex **2**. In summary, this research shows that the assembly of dipyridyl ligands with an optically active BINOL connector and metal ions offers an attractive and promising route to generate unique structural motifs that cannot be obtained with other types of normal,

rigid or flexible *exo*-bidentate organic ligands, such as 4,4′-bipy and related organic ligands.

Experimental Section

General: All chemicals were commercially available and were used as received without further purification. (*S*)-L and (*R*)-L were synthesized according to a literature method.[9d] The measurement of the optical rotation was performed with a Polarimeter 341. ESI mass spectra were recorded with a Fisons VG platform. The IR spectra (KBr disk) were recorded with a Magna 750 FTIR spectrophotometer. Elemental analyses were determined with an Elementar Vario ELIII elemental analyzer.

Preparation of [Ag{(*S*)-L}(ClO_4)]$_n$ (1): A solution of $AgClO_4 \cdot H_2O$ (0.021 g, 0.1 mmol) in H_2O (5 mL) was added slowly to a stirred solution of (*S*)-L (0.047 g, 0.1 mmol) in MeCN (10 mL). The reaction mixture was stirred at 60 °C for 3 h and then filtered. Colorless crystals of complex **1** were obtained by allowing the filtrate to evaporate slowly in air for two weeks. Yield (0.062 g, 92%). $C_{32}H_{24}AgClN_2O_6$ (675.9): calcd. C 56.81, H 3.55, N 4.14; found C 56.84, H 3.52, N 4.17. IR (KBr pellet): $\tilde{\nu}$ = 3583 (m, br), 3062 (m), 2922 (m), 1943 (vw), 1672 (vw), 1618 (s), 1592 (s), 1563 (m), 1505 (s), 1466 (w), 1446 (m), 1429 (s), 1357 (vw), 1324 (s), 1287 (s), 1269 (s), 1215 (s), 1151 (vw), 1073 (s, br), 1021 (m), 960 (w), 914 (w), 860 (vw), 804 (m), 746 (m), 669 (vw), 619 (m), 573 (vw), 497 (w), 458 (w), 422 cm^{-1} (w).

Preparation of [Ag{(*R*)-L}(ClO_4)]$_n$ (2): The procedure was similar to the synthesis of complex **1**, except that (*R*)-L was used instead of (*S*)-L. Yield (0.057 g, 84%). $C_{32}H_{24}AgClN_2O_6$ (675.9): calcd. C 56.81, H 3.55, N 4.14; found C 56.89, H 3.63, N 4.16. IR (KBr pellet): $\tilde{\nu}$ = 3585 (m, br), 3060 (m), 2922 (m), 1942 (vw), 1670 (w), 1617 (s), 1592 (s), 1563 (w), 1505 (s), 1468 (w), 1446 (m), 1428 (s), 1356 (w), 1321 (s), 1287 (s), 1269 (s), 1216 (s), 1151 (vw), 1091 (s, br), 1020 (s), 959 (w), 912 (w), 861 (vw), 804 (m), 747 (m), 670 (w), 619 (m), 573 (vw), 497 (w), 459 (w), 422 cm^{-1} (w).

Preparation of [(Cd{(*S*)-L}(H_2O)Cl_2)(H_2O)$_{0.5}$]$_n$ (3): A solution of (*S*)-L (0.047 g, 0.1 mmol) in MeOH (5 mL) was carefully layered on a solution of $CdCl_2 \cdot 2.5H_2O$ (0.023 g, 0.1 mmol) in H_2O (5 mL). Diffusion between the two phases over a period of two weeks produced colorless crystals of **3**. Yield (0.047 g, 69%). $C_{32}H_{27}CdCl_2N_2O_{3.5}$ (678.9): calcd. C 56.56, H 4.00, N 4.12; found C 56.58, H 4.03, N 4.13. IR (KBr pellet): $\tilde{\nu}$ = 3402(m, br), 3053 (m), 2923 (m), 1952 (vw), 1747 (vw), 1619 (s), 1593 (s), 1562(m), 1504 (s), 1467 (w), 1446 (m), 1426 (s), 1356 (w), 1321 (s), 1287 (s), 1268 (s), 1214 (s), 1151 (w), 1089 (s), 1065 (s), 1017 (s), 959 (w), 913 (w), 860 (vw), 803 (s), 746 (m), 669 (vw), 619 (m), 573 (w), 497 (w), 458 (w), 422 cm^{-1} (m).

Preparation of [(Zn{(*S*)-L}Cl_2)(DMF)$_{0.5}$(H_2O)$_{0.5}$]$_n$ (4): A solution of $ZnCl_2$ (0.07 g, 0.1 mmol) in DMF (10 mL) was added slowly to a stirred solution of (*S*)-L (0.047 g, 0.1 mmol) in MeCN (10 mL). The reaction mixture was stirred at 60 °C for 6 h and then filtered. Colorless crystalline complex **4** was obtained in high yield by slow diffusion of diethyl ether into the filtrate over several days. Yield (0.058 g, 89%). $C_{33.5}H_{28.5}Cl_2N_{2.5}O_3Zn$ (650.4): calcd. C 61.86, H 4.38, N 5.38; found C 61.75, H 3.30, N 5.33. IR (KBr pellet): $\tilde{\nu}$ = 3048 (w), 2925 (w), 2858 (w), 1665 (s), 1624 (s), 1594 (m), 1567 (w), 1511 (m), 1384 (w), 1358 (vw), 1322 (m), 1276 (s), 1240 (m), 1219 (m), 1153 (m), 1091 (s), 1066 (s), 1030 (m), 963 (w), 917 (w), 871 (vw), 815 (s), 754 (m), 666 (vw), 636 (w), 605 (vw), 492 (w), 456 (vw), 430 cm^{-1} (vw).

[(Pd_2{(*S*)-L}$_2Cl_4$)(H_2O)$_{1.5}$]$_n$ (5): A solution of [$PdCl_2$(cod)] (0.12 g, 0.1 mmol) in CH_2Cl_2 (5 mL) was added slowly to a stirred solution of (*S*)-L (0.047 g, 0.1 mmol) in CH_2Cl_2 (5 mL). The reaction mixture was stirred at reflux temperature under nitrogen for 3 h and was then evaporated under reduced pressure. Yellow crystals of complex **5** were obtained by slow diffusion of hexane into the resultant solution over several days. Yield (0.055 g, 83%). $C_{64}H_{51}Cl_4N_4O_6Pd_2$ (1326.7): calcd. C 57.94, H 3.84, N 4.21; found C 57.98, H 3.91, N 4.25. IR (KBr pellet): $\tilde{\nu}$ = 3412 (m, br), 3055 (m), 2921 (m), 1925 (vw), 1743 (vw), 1617 (s), 1592 (s), 1563 (m), 1506 (s), 1462 (w), 1445 (m), 1428 (m), 1363 (vw), 1324 (s), 1281

Table 3. Crystallographic data for complexes **1**–**5**

Compound	**1**	**2**	**3**	**4**	**5**
Formula	$C_{32}H_{24}AgClN_2O_6$	$C_{32}H_{24}AgClN_2O_6$	$C_{32}H_{27}CdCl_2N_2O_{3.5}$	$C_{33.5}H_{28.5}Cl_2N_{2.5}O_3Zn$	$C_{64}H_{51}Cl_4N_4O_6Pd_2$
Mol. mass	675.85	675.85	678.86	650.36	1326.69
Crystal size [mm]	0.48 × 0.35 × 0.20	0.40 × 0.20 × 0.20	0.58 × 0.25 × 0.15	0.40 × 0.36 × 0.34	0.38 × 0.14 × 0.12
Crystal system	monoclinic	monoclinic	monoclinic	orthorhombic	monoclinic
Space group	C_2	C_2	C_2	$P2_12_12_1$	$P2_1$
a [Å]	24.984(4)	25.135(4)	25.704(5)	11.2955(13)	16.177(5)
b [Å]	7.2818(12)	7.3173(13)	7.1752(13)	16.5633(19)	9.248(3)
c [Å]	17.170(3)	17.101(3)	17.089(3)	19.966(2)	20.061(6)
β [°]	104.245(5)	104.390(4)	105.375(4)		96.901(6)
V [Å^3]	3027.7(9)	3046.5(9)	3038.9(9)	3735.4(7)	2979.6(15)
Z	4	4	4	4	2
D_c [g cm^{-3}]	1.483	1.474	1.484	1.156	1.470
μ [mm^{-1}]	0.800	0.795	0.931	0.832	0.836
F(000)	1368	1368	1372	1340	1334
T [K]	293(2)	294(2)	294(2)	293(2)	294(2)
λ(Mo-K_α) [Å]	0.71073	0.71073	0.71073	0.71073	0.71073
Flack parameters (x)	0.01(4)	0.01(4)	0.27(18)	0.03(3)	0.19(8)
Reflns. collected	10262	10312	10340	25626	19783
Unique reflns.	6430	6454	6421	8586	13048
Obsd. reflns. [F>4.0σ(F)]	4289	4000	4289	2297	5955
Parameters	379	379	370	401	717
S on F^2	0.979	0.921	0.959	0.945	1.030
R_1	0.0546	0.0554	0.0479	0.0799	0.0717
wR	0.1622	0.1654	0.1160	0.2405	0.281
$\Delta\rho_{min}$ and $\Delta\rho_{max}$ [e·Å^{-3}]	0.879 and –0.608	0.866 and –0.567	0.866 and –0.428	0.823 and –0.380	0.996 and –0.982

(s), 1274 (m), 1216 (m), 1154 (vw), 1092 (s), 1066 (m), 1023 (m), 914 (w), 862 (vw), 806 (s), 748 (m), 676 (vw), 610 (m), 573 (w), 523 (w), 456 (w), 421 cm^{-1} (m).

X-ray Crystallography: Intensity data for the five complexes were recorded on a Siemens Smart CCD diffractometer with graphite-monochromated Mo-K_α radiation (λ = 0.71073 Å) at room temperature. Empirical absorption corrections were applied with the SADABS program.[12] The structures were solved by direct methods and all calculations were performed using the SHELXL-97 program.[13] The positions of the H atoms in complexes **1**–**5** were generated geometrically (C–H bond fixed at 0.96 Å) and assigned isotropic thermal parameters, and allowed to ride on their parent carbon atoms before the final cycle of refinement. The structures were refined by full-matrix least-squares minimization of $\Sigma(F_o - F_c)^2$ with anisotropic thermal parameters for all atoms except the H atoms. The crystallographic data for complexes **1**–**5** are listed in Table 3.

CCDC-240015 to -240019 (for **1**–**5**, respectively) contain the supplementary crystallographic data for this paper. These data can be obtained free of charge from The Cambridge Crystallographic Data Centre via www.ccdc.cam.ac.uk/data_request/cif.

Acknowledgments

We thank the Hong Kong Research Grants Council (project no. PolyU5306/01P), The University Grants Committee Area of Excellence Scheme in Hong Kong (AoE P/10-0), and the Hong Kong Polytechnic University Area of Strategic Development Fund for financial support of this study.

[1] a) J. M. Lehn, *Supramolecular Chemistry: Concepts and Perspectives*; VCH, Weinheim, **1995**; b) J. W. Steed, J. L. Atwood, *Supramolecular Chemistry*, J. Wiley and Sons, New York, **2000**.

[2] a) B. J. Holliday, C. A. Mirkin, *Angew. Chem. Int. Ed.* **2001**, *40*, 2022–2043; b) S. Leininger, B. Olenyuk, P. J. Stang, *Chem. Rev.* **2000**, *100*, 853–907; c) M. Eddaoudi, D. B. Moler, H. Li, B. Chen, T. M. Reineke, M. O'Keeffe, O. M. Yaghi, *Acc. Chem. Res.* **2001**, *34*, 319–330; d) N. R. Champness, D. A. Lemenovskii, A. G. Majouga, N. V. Zyk, M. Schröder, *Coord. Chem. Rev.* **2001**, *222*, 155–192.

[3] a) M. A. Masood, E. J. Enemark, T. D. P. Stack, *Angew. Chem. Int. Ed.* **1998**, *37*, 928–932; b) C. M. Hartshorn, P. J. Steel, *Chem. Commun.* **1997**, 541–542; c) J. Schneider, M. Köckerling, R. Kopitzky, G. Henkel, *Eur. J. Inorg. Chem.* **2003**, 1727–1734.

[4] a) U. Knof, A. von Zelewsky, *Angew. Chem. Int. Ed.* **1999**, *38*, 302–322; b) M. Albrecht, *Chem. Rev.* **2001**, *101*, 3457–3497; c) F. A. A. Paz, Y. Z. Khimyak, A. D. Bond, J. Rocha, J. Klinowski, *Eur. J. Inorg. Chem.* **2002**, 2823–2828.

[5] See for example: a) M. Munakata, L. P. Wu, T. Kuroda-Sowa, *Adv. Inorg. Chem.* **1999**, *46*, 173–303; b) A. J. Blake, N. R. Champness, S. S. M. Chung, W. S. Li, R. P. Schröder, *Chem. Commun.* **1997**, 1005–1006; c) T. L. Hennigar, D. C. MacQuarrie, P. Losier, R. D. Rogers, M. J. Zaworotko, *Angew. Chem. Int. Ed. Engl.* **1997**, *36*, 972–973; d) E. Bermejo, R. Carballo, A. Castineiras, R. Dominguez, A. E. Liberta, C. Maichle-Moessmer, M. M. Salberg, D. X. West, *Eur. J. Inorg. Chem.* **1999**, 965–973; e) Y. B. Dong, R. C. Layland, M. D. Smith, N. G. Pschirer, U. H. F. Bunz, H. C. zur Loye, *Inorg. Chem.* **1999**, *38*, 3056–3060; f) G. D. Munno, F. Cipriani, D. Armentano, M. Julve, J. A. Real, *New J. Chem.* **2001**, *25*, 1031–1036; g) M. Maekawa, H. Konaka, Y. Suenaga, T. Kuroda-Sowa, M. Munakata, *J. Chem. Soc. Dalton Trans.* **2000**, 4160–4166; h) K. Uemura, S. Kitagawa, M. Kondo, K. Fukui, R. Kitaura, H. C. Chang, T. Mizutani, *Chem. Eur. J.* **2002**, *8*, 3586–3600.

[6] See for example: a) K. Biradha, Y. Hongo, M. Fujita, *Angew. Chem. Int. Ed.* **2000**, *39*, 3843–3845; b) D. K. Chand, K. Biradha, M. Fujita, *Chem. Commun.* **2001**, 1652–1653; c) K. Biradha, M. Fujita, *Chem. Commun.* **2002**, 1877–1878; d) S. Banfi, L. Carlucci, E. Caruso, G. Ciani, D. M. Proserpio, *J. Chem. Soc. Dalton Trans.* **2002**, 2714–2721.

[7] a) R. Horikoshi, T. Mochida, H. Moriyama, *Inorg. Chem.* **2002**, *41*, 3017–3024; b) D. Braga, M. Polito, M. Bracaccini, D. D'Addario, E. Tagliavini, D. M. Proserpio, F. Grepioni, *Chem. Commun.* **2002**, 1080–1081.

[8] a) M. C. Hong, Y. J. Zhao, W. P. Su, R. Cao, M. Fujita, Z. Y. Zhou, A. S. C. Chan, *J. Am. Chem. Soc.* **2000**, *122*, 4819–4820; b) M. C. Hong, Y. J. Zhao, W. P. Su, R. Cao, M. Fujita, Z. Y. Zhou, A. S. C. Chan, *Angew. Chem. Int. Ed.* **2000**, *39*, 2468–2470; c) Y. J. Zhao, M. C. Hong, W. P. Su, R. Cao, Z. Y. Zhou, A. S. C. Chan, *Chem. Lett.* **2000**, 28–29; d) R. H. Wang, M. C. Hong, W. P. Su, Y. C. Liang, R. Cao, Y. Z. Zhao, J. B. Weng, *Bull. Chem. Soc. Jpn.* **2002**, *75*, 725–730; e) M. C. Hong, W. P. Su, R. Cao, M. Fujita, J. X. Lu, *Chem. Eur. J.* **2000**, *6*, 427–432.

[9] a) R. Noyori, *Angew. Chem. Int. Ed.* **2002**, *41*, 2008–2022; b) L. Pu, *Chem. Rev.* **1998**, *98*, 2405–2494; c) J. K. Whitesell, *Chem. Rev.* **1989**, *89*, 1581–1590; d) R. H. Wang, L. J. Xu, X. S. Li, Y. M. Li, Q. Shi, Z. Y. Zhou, M. C. Hong, A. S. C. Chan, *Eur. J. Inorg. Chem.* **2004**, 1595–1599.

[10] a) S. J. Lee, W. Lin, *J. Am. Chem. Soc.* **2002**, *124*, 4554–4555; b) Y. Cui, S. J. Lee, W. Lin, Y. *J. Am. Chem. Soc.* **2003**, *125*, 6014–6015; c) Y. Cui, H. L. Ngo, P. S. White, W. Lin, *Chem. Commun.* **2003**, 994–995; d) Y. Cui, O. R. Evans, H. L. Ngo, P. S. White, W. Lin, *Angew. Chem. Int. Ed.* **2002**, *41*, 1159–1162; e) A. Lützen, M. Hapke, J. Griep-Raming, D. Haase, W. Saak, *Angew. Chem. Int. Ed.* **2002**, *41*, 2086–2089; f) M. Kimura, M. Sano, T. Muto, K. Hanabusa, H. Shirai, *Marcromolecules* **1999**, *32*, 7951–7953.

[11] E. P. Kyba, G. W. Gokel, F. de Jong, K. Koga, L. R. Sousa, M. G. Siegel, L. Kaplan, G. D. Y. Sogah, D. J. Cram, *J. Org. Chem.* **1977**, *42*, 4173–4184.

[12] G. M. Sheldrick, *SADABS*, Program for Empirical Absorption Correction of Area Detector Data, University of Göttingen, Germany, **1996**.

[13] G. M. Sheldrick, *SHELXS 97*, Program for Crystal Structure Solution, University of Göttingen, Germany, **1997**.

Received: July 28, 2004